Simulations of ion cyclotron emission from DIII-D tokamak plasmas

A I Zalzali[1], K E Thome[2], R O Dendy[3,1], B Chapman[3], S C Chapman[3], J W S Cook[3],
M A Van Zeeland[2], N A Crocker[4], and G H DeGrandchamp[5]

[1]*Centre for Fusion, Space and Astrophys., Dept. Phys., U. Warwick, Coventry CV4 7AL, UK*

[2]*General Atomics, San Diego, CA 92121, USA*

[3]*CCFE, Culham Science Centre, Abingdon, OX14 3DB, UK*

[4]*Department of Physics and Astronomy, UCLA, Los Angeles CA 90095, USA*

[5]*Department of Physics and Astronomy, UC Irvine, Irvine CA 92697, USA*

1. Introduction

Ion cyclotron emission (ICE) comprises strongly suprathermal radiation, typically with multiple narrow spectral peaks at ion cyclotron harmonics. ICE is driven by the magnetoacoustic cyclotron instability (MCI), caused by a spatially localised inversion in the velocity-space distribution of the minority energetic ions[1-5]. Recent observations[6,7] from H-mode deuterium plasmas heated by deuterium neutral beam injection (NBI) in DIII-D, were obtained using the Ion Cyclotron Emission diagnostic[8], which has been recently upgraded [9]. The experiments show spectral peaks at the local deuteron ion cyclotron frequency f_{ci} in the DIII-D edge plasma, and its harmonics. We have run direct numerical simulations, using the EPOCH particle-in-cell (PIC) code[3-5,10], for these DIII-D ICE scenarios for the first time. We initialize our EPOCH PIC simulation with a majority thermal deuteron plasma, a small minority population of energetic 75 keV perpendicular-injected NBI deuterons, and a neutralising population of thermal electrons. The initial velocity distribution of the NBI deuterons is modelled as a ring-beam; this approach has been successful in capturing the physics underlying ICE observations under different NBI plasma conditions in the KSTAR tokamak[11] and LHD stellarator[12,13]. EPOCH solves[10] the Maxwell-Lorentz system of equations for fully kinetic electrons and ions, together with their self-consistent electric and magnetic fields. Importantly, particle gyro-orbits are fully resolved, hence all aspects of cyclotron resonance phenomenology are captured from first principles. The plasma parameters match those of the experiment (DIII-D shot 166357), except that we use a higher ratio of the number densities of NBI ions to thermal ions ($n_{NBI}/n_i = 10^{-2}$), to achieve acceptable computational run times. The scaling consequences of this choice are understood[5] and do not affect the key physics. We combine our numerical approach with evaluation of the analytical linear growth rates of the MCI in the experimentally relevant parameter regime. We have applied the same procedure to a classic case of edge ICE from JET[4], leading to physically interesting comparisons. Our aim is to use powerful computational techniques, coupled with high performance computations, to demonstrate that ICE signals can be used to infer the characteristics of fast-ion velocity distribution functions. This supports the further exploitation of ICE as a diagnostic tool to study energetic particles in fusion reactors.

2. Simulation results and comparison with DIII-D ICE

Figure 1 plots the energy flow in our PIC simulation, as the energetic minority NBI ion population relaxes within the majority thermal plasma under self-consistent Maxwell-Lorentz dynamics. Taken together, the time traces of the change of energy density of the self-consistent magnetic $(\Delta B_z)^2$ and electrostatic $(E_x)^2$ field components, as well as the change in kinetic energy density of the electrons (KE_e), majority (KE_i) and minority (KE_{min}) ion species, confirm that the MCI arises as an emergent property. We observe an energy shift from the NBI deuterons

primarily to the thermal background ions (red curve), with a smaller fraction of the energy shifted to the background electrons.

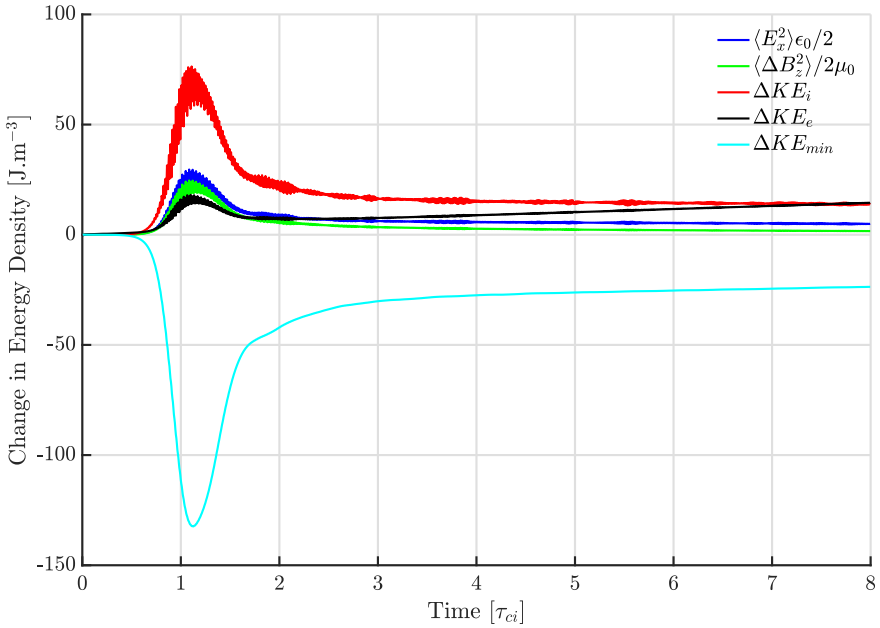

Fig.1 Time evolution of the change in energy density of particles together with the electric and magnetic fields, from an EPOCH simulation with a 75keV minority NBI deuteron population. The plasma parameters correspond to those obtained during the experiment at $\rho = R/a \approx 1.2$, where R is the major radius and a is the minor radius of the tokamak: $n_e = 9\times10^{18}$m^{-3}, $n_{NBI}/n_i = 10^{-2}$, $T_e = 84$eV, $T_i = 321$eV, $B_{0z} = 1.33$T, and.
The simulation spans $0 < x < 300{,}000\ \lambda_D$ and $0 < t < 18\tau_{cD}$. Top (red) Change in kinetic energy density of the thermal bulk plasma deuterons; (blue) energy density of the electrostatic field E_x; (black) change in energy density of the electrons; (green) energy density of the magnetic field perturbation ΔB_z; (cyan) change in kinetic energy density of the minority energetic NBI deuterons. Time is normalised to the deuteron gyroperiod τ_{cD}. For clarity, the change of energy density in this figure is shown up to $8\tau_{cD}$ but the simulation is allowed to continue running for $18\tau_{cD}$ in order to collect more data.

Figure 2a shows the spatiotemporal Fourier transform of the spectral density of the excited magnetic field $(\Delta B_z)^2$. The dominant field excitations arising from the MCI are at the intersection of the fast Alfvén branch $\omega \approx kV_A$, where V_A denotes the Alfvén speed, and the multiple horizontal cyclotron harmonic waves. We note that the degeneracy of these two classes of normal mode at their intersection in (ω,k) space is encompassed by the generalised analytical solution of the linear mode conversion regime of two independent modes of oscillation in a plasma medium. A wave-mechanical approach[14] to solving the local approximate dispersion relation of the system $[\omega - \omega_1(\mathrm{x},\mathrm{k})][\omega - \omega_2(\mathrm{x},\mathrm{k})] = \eta$, generates the solutions $(\omega_\pm)$, plotted in Fig. (2b). The mode coupling, symbolized by η, is a small quantity that is only significant in the neighbourhood of the coupling point and whose presence leads to the characteristic shape of the dispersion curves at successive intersections of ω_1 and ω_2, which correspond here to the fast Alfvén and cyclotron harmonic wave branches.

To obtain a frequency spectrum, we integrate the spatiotemporal Fourier transform in Fig.2(a) over the wavenumber domain. This is plotted as the blue trace in Fig.3, to be compared with the experimental spectrum from DIII-D #166357[6] (red trace); the green trace defines the noise level. Our simulated spectrum exhibits distinct spectral peaks at integer cyclotron harmonics up to $7\ f_{ci}$. This is in good agreement with the observed ICE spectrum, for example the dominant spectral peak in both cases is the third harmonic. Furthermore the simulation replicates the relative strengths of the observed ICE spectral peaks at the second, third and fourth harmonics.

In order to quantify the computational noise, and verify that the presence of the NBI ions has indeed triggered the excitation of the MCI with its ICE-like power spectrum, we have run an identical high resolution EPOCH simulation of the background plasma in the absence of the NBI ions. The corresponding power spectrum (green trace) thus defines the level at which the normal modes of the system are populated by noise, through the fluctuation-dissipation theorem, in the absence of drive from energetic ions. Taken together, the three traces in Fig.3 strongly suggest that the first principles physics in our simulation, from which the MCI emerges, is responsible for the observed ICE.

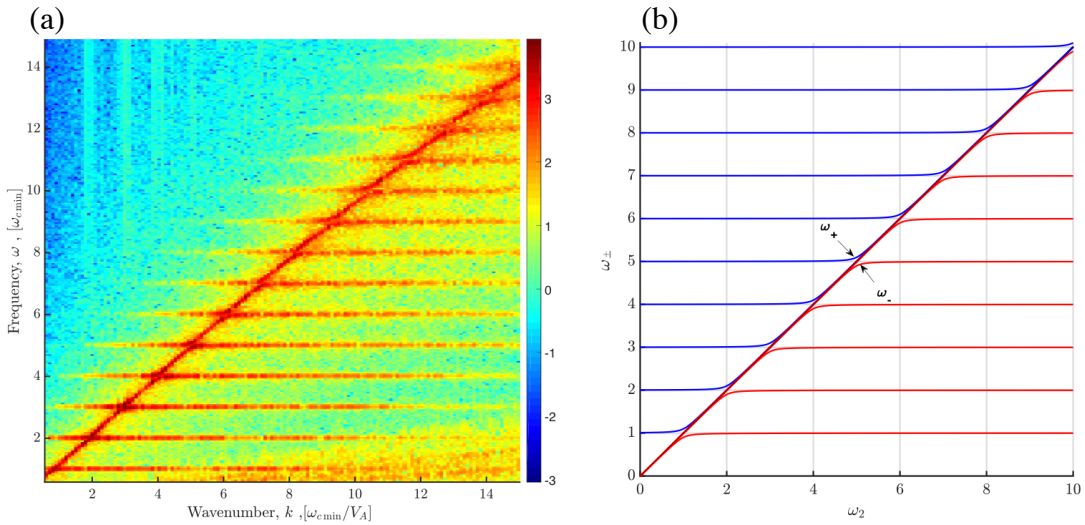

Fig.2 (a, Left) Distribution of energy in the oscillatory part ΔB_z of the B_z field component across frequency-wavenumber space, spanning the first 15 cyclotron harmonics and corresponding dimensionless wavenumber $k\ \omega_{cmin}/v_A$. Shading indicates the $\log_{10}$ of the spectral density. **(b, Right)** A wave-mechanical approach[14] to linear mode conversion using the system $\hat{L}\Psi = i\partial\Psi/\partial t$, where $\hat{L}$ is Hermitian operator whose solution generates the eigenvalues $\omega_{\pm}$, plotted in this figure as a function of ω_2. The underlying structure matches that obtained in (a).

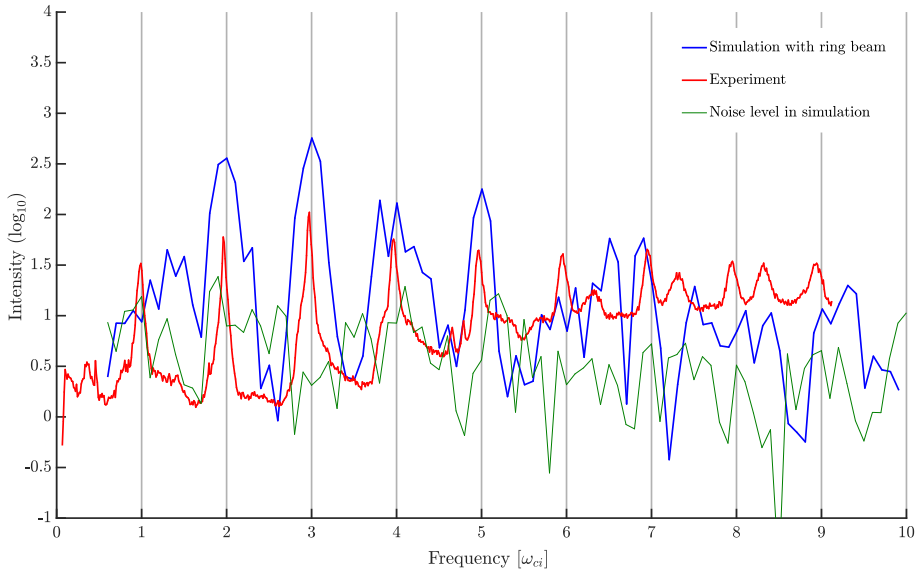

Fig.3 Spectral intensity of ICE. Blue trace: output of the PIC simulation of the spectral intensity of the fluctuating B_z field energy density. Red trace: the measured spectral intensity of ICE from the NBI-heated DIII-D H-mode deuterium plasma [6]. Green trace: the noise baseline obtained by running a simulation without the NBI ions.

3. Comparison of linear MCI growth rates in DIII-D and JET ICE cases

Figure 4 plots the analytical linear growth rate of the MCI, obtained from Eq.(8) of Ref.[2], for the experimental parameter sets for two cases of observed ICE from tokamak edge plasmas.

These cases are the DIII-D shot #166357 already considered in this report, and JET deuterium-tritium plasma 26148[15]. The latter is fully consistent with earlier calculations[3-5], which show that harmonics below the sixth are linearly stable. As discussed in Refs.[3-5], the observed ICE peaks at lower harmonics < 6 in JET arise from nonlinear interactions between pairs of spectral peaks linearly excited at harmonics > 6. In contrast, in the DIII-D case, we find that the MCI is linearly excited down to the second harmonic. Furthermore the relative strength of MCI linear growth rates at the second, third and fourth ion cyclotron harmonics is the same as in the observed ICE spectrum. This suggests that in the DIII-D case, the saturated ICE spectrum is more strongly conditioned by the properties of the linear MCI than the JET case. As a corollary, it suggests that nonlinear MCI physics may be less important for the DIII-D case.

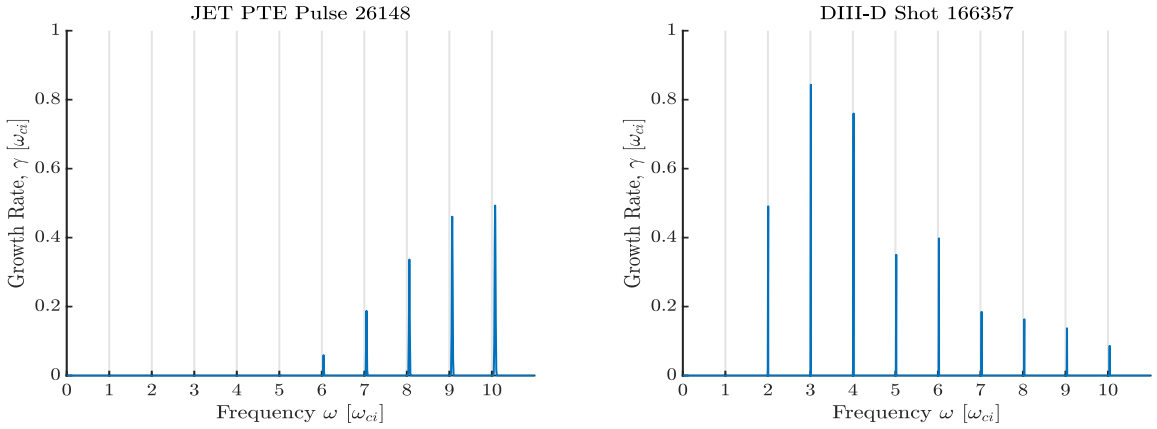

Fig.4 Linear analytical growth rates of the MCI as a function of frequency, obtained from Eq.(8) of Ref.[2], for (a, Left) JET PTE Pulse 26148[15] and (b, Right) DIII-D shot 166357[6].

4 Conclusions

The DIII-D ICE spectrum considered here[6] is evidently driven by the magnetoacoustic cyclotron instability of perpendicular-injected 75 keV NBI deuterons in the outer midplane edge plasma. It is within the genre of NBI-driven edge ICE in KSTAR[11] and LHD[12,13]. We have established points of contact with ICE driven by fusion products in JET[15], and explored ICE driven by NBI ions to support the current ongoing research at DIII-D[7,9].

[1] R O Dendy, C N Lashmore-Davies, K G McClements & G A Cottrell, *Phys. Plasmas* **1**, 1918 (1994)
[2] K G McClements, R O Dendy, C N Lashmore-Davies, G A Cottrell *et al*., *Phys. Plasmas* **3**, 543 (1996)
[3] J W S Cook, R O Dendy & S C Chapman, *Plasma Phys. Control. Fusion* **55**, 065003 (2013)
[4] L Carbajal, R O Dendy, S C Chapman & J W S Cook, *Phys. Plasmas* **21**, 012106 (2014)
[5] L Carbajal, R O Dendy, S C Chapman and J W S Cook, *Phys. Rev. Lett.* **118**, 105001 (2017)
[6] K E Thome, D C Pace, R I Pinsker, M A Van Zeeland *et al*., *Nucl. Fusion* **59**, 086011 (2019)
[7] N A Crocker, S X Tang, K E Thome et al., 28th IAEA FEC, paper IAEA-EX/P1-920 (2021)
[8] K E Thome, D C Pace, R I Pinsker, O Meneghini *et al*., *Rev. Sci. Instrum.* **89**, 10I102 (2019)
[9] G H DeGrandchamp, K E Thome, W W Heidbrink, *et al*., *Rev. Sci. Instrum.* **92(3)**, 033543 (2021)
[10] T D Arber, K Bennett, C S Brady *et al*., *Plasma Phys. Control. Fusion* **57**, 113001 (2015)
[11] B Chapman, R O Dendy, S C Chapman, K G McClements, G S Yun *et al*., *Nucl. Fusion* **59**, 106021 (2019)
[12] B C G Reman, R O Dendy, T Akiyama *et al*., *Nucl. Fusion* **59**, 096013 (2019)
[13] B C G Reman, R O Dendy, T Akiyama, S C Chapman, *et al*., *Nucl. Fusion* **61**, accepted (2021)
[14] R O Dendy, *Phys. Fluids* **31**, 298 (1988)
[15] G A Cottrell, V P Bhatnagar, O da Costa, R O Dendy, J Jacquinot *et al*., *Nucl. Fusion* **33**, 1365 (1993)

This work received support from the RCUK Energy Programme grant no. EP/T012250/1. It was carried out within the framework of the EUROfusion Consortium and has received funding from the Euratom research and training programme 2014-2018 and 2019-2020 under grant agreement No 633053. The views and opinions expressed herein do not necessarily reflect those of the European Commission. This material is based upon work supported by the U.S. Department of Energy, Office of Science, Office of Fusion Energy Sciences, using the DIII-D National Fusion Facility, a DOE Office of Science user facility, under Awards DE-FC02-04ER54698 and DE-SC0020337.